*Mathematical Biosciences and Engineering*

http://www.aimspress.com/journal/mbe

MBE, 20(1): 296–317.
DOI: 10.3934/mbe.2023014
Received: 07 July 2022
Revised: 07 September 2022
Accepted: 08 September 2022
Published: 08 October 2022

*Research article*

# Discrete models for analyzing the behavior of COVID-19 pandemic in the State of Mexico, Mexico

**Erik A. Vázquez Jiménez[1,*], Jesús Martínez Martínez[1,*], Leonardo D. Herrera Zuniga[2,*] and J. Guadalupe Reyes Victoria[3,*]**

[1] Tecnologico de Estudios Superiores de Huixquilucan-TESH, Estado de Mexico, Mexico
[2] Universidad Autonoma del Estado de Morelos, Estado de Morelos, Mexico
[3] Universidad Autonoma Metropolitana, Unidad Iztapalapa, CP 09340, Cd. de Mexico, Mexico

* **Correspondence:** Email: k_i_res@hotmail.com, division.mecatronica@huixquilucan.tecnm.mx, ldhz04@gmail.com, revg@xanum.uam.mx.

**Abstract:** In this paper we analyze the behavior of the COVID-19 pandemic during a certain period of the year 2020 in the state of Mexico, Mexico. For this, we will use the discrete models obtained by the first, third and fourth authors of this work. The first is a one-dimensional model, and the second is two-dimensional, both non-linear. It is assumed that the population of the state of Mexico is constant and that the parameters used are the infection capacity, which we will initially assume to be constant, and the recovery and mortality parameters in that state. We will show that even when the statistical data obtained are disperse, and the process could be stabilized, this has been slow due to chaotic mitigation, creating situations of economic, social, health and political deterioration in that region of the country. We note that the observed results of the behavior of the epidemic during that period for the first variants of the virus have continued to be observed for the later variants, which has not allowed the eradication of the pandemic.

**Keywords:** pandemic; two dimensional discrete dynamics; attractor-repulser fixed points; mitigation; Chaos; eradication

## 1. Introduction

The COVID-19 pandemic that Mexico and the world in general is experiencing, since 2020, has led a large number of scientists to try solving the problem from different points of view and showing the scope it has within the economy, society, health and politics [1–8]. In particular, mathematicians around the world have responded by formulating models that have helped to partially understand the behavior of the infectious process at least in the first months since its appearance. Such models have

followed the fundamental model called **SIR** by Kerman and Kendrick [9] by means of systems of differential equations. Many papers have been written modifying these primary systems throughout this period. However, the solutions obtained or approximated have not been able to give a satisfactory answer to the process, since in most cases their predictions are asymptotic and propose a stabilization and eradication of the pandemic, which has not happened to this day. The point is that the behavior of the solutions obtained is very simple in the configuration space, and it is not possible to observe at times the so-called outbreaks (as in Europe) or the chaotic behavior (as in America) of such process. On the other hand, several researchers in different parts of the world have proposed various models using discrete dynamics to study the behavior of the epidemic and have obtained partial, but altogether valuable results [10–15]. In our case, following the same line of research, we have preferred to use the analysis carried out by Reyes et al. in [16] using two discrete dynamic systems that allow one, from the first, one-dimensional, simple case, to predict chaotic behaviors of the process, because the homology of the solutions is richer than in the continuous case. The two-dimensional case proposed there shows a clearer approach to the process that continues to occur even to this day.

In this work we show the use of the model in [16] to study the behaviour of the epidemic process in the State of Mexico, Mexico, in 2020, using the proposed parameters and with statistical data obtained from reliable and relevant sources. We reiterate that this work is objectively theoretical by virtue of the fact that the data obtained in general by government agencies and institutes are not satisfactorily real, and for the problem of the epidemic it must necessarily be of this type to carry out a prevention project. We emphasize that in the period in which the model shown here was applied, there were still no vaccines, and the mitigation was carried out with isolations and contagion prevention methods in the region studied. However, the behavior of the epidemic for the following variants followed a similar route [1–4, 17, 19], sometimes weaker but still having repercussions on the economy, and social, health and political aspects.

The paper is organized as follows. We start in Section 2 by establishing the results in the simplest and most understandable way for a wide range of readers. In Section 3, we give the basic elements of the theory used for one-dimensional dynamical systems generated the classic quadratic family. In Section 4 we use the statistical data obtained for the pandemic in the state of Mexico, and we analyze it for the case when the used parameters are constant. In Section 5 we give the elements that define a chaotic one-dimensional dynamic system, and we use them in Section 6 to model a mitigation function for the basic contagion numbers with the data obtained for this Mexican state, which is chaotic in the first 12 months of contagion. Finally, in Section 7, using the mitigation function obtained, we define a two-dimensional dynamic system coupling it with the quadratic family, obtaining information on the eradication of a pandemic with weak chaos in this region of Mexico.

## 2. The main results

In this section we establish the main results of this work concerning the behavior of the pandemic in Result 1 for the case without mitigation and in Result 2 for the case in which preventive measures were taken in the analyzed period, leaving the proofs in Sections 4 and 6 respectively.

**Result 1.** *The epidemic in the state of Mexico would have been stabilized (flattening the contagion curve) in the period of 2020–2021 in a natural way with the condition that both the basic contagion number, and the recovery and mortality parameters had remained constant.*

**Result 2.** *With the prevention policies applied for mitigation in the State of Mexico during the period from April to October 2020, the behavior of the pandemic in that region, although globally it was weakly chaotic, was eradicated slowly for almost all (in the topological and measurable senses) the initial conditions in the number of infected individuals and in the contagion capacity.*

## 3. The early one dimensional discrete model of prevention without mitigation

In this section we mention the necessary minimum number of elements [18] for the study of the first analysis, in the same way in which they were established in [16], with the aim of showing the possible current scenarios of the pandemic obtained with this model, assuming a constant contagion capacity. Also, we assume here, for simplicity, a closed population having a total number of (unknown) individuals $N_\infty$ [20].

### *3.1. The modified logistic discrete model*

In this work we denote the parameters of the contagion problem by

$$\begin{aligned} \frac{R_0}{N_\infty} &= \text{Probability of contagion of the population,} \\ \alpha &= \text{Probability of recovery of the population,} \\ \beta &= \text{Rate of mortality of the population,} \end{aligned}$$

subject to the conditions

$$0 \leq \frac{R_0}{N_\infty}, \alpha, \beta \leq 1 \quad \text{and} \quad 0 < \alpha + \beta < 1, \tag{3.1}$$

where $R_0$ is the number of individuals that can be infected by an already infected one, usually known as the *basic reproductive number* (at time $t = 0$) in the epidemiological literature [21, 22].

We will use here a modified logistic discrete model of May [23] and a fortnight as a unit of time, since in general it is the time in which the symptoms of COVID-19 appear after the contagion.

With these values in mind, if $N_t$ denotes the number of total real infected individuals (not accumulated, including asymptomatic and suspected ones, because even when their values are unknown, together with the recovered ones that may recur, these are vectors for the next generation of infected ones) at time $t \in \mathbb{N} = \{0, 1, 2, \ldots\}$ after the epidemic begins, then, for constant $R_0$,

$$N_{t+1} = \frac{R_0}{N_\infty} N_t(N_\infty - N_t) - \alpha N_t - \beta N_t \tag{3.2}$$

models the number of infected ones at time $t + 1$, i.e., a unit of time after.

Here, the expression $\alpha N_t + \beta N_t$ acts, at first, as a control function to counterweight the contagion expression $\frac{R_0}{N_\infty} N_t(N_\infty - N_t)$.

For the analysis of the dynamics of the unidimensional non-linear System (3.2), we use the properties of the function

$$f(N_t) = N_{t+1} = \frac{R_0}{N_\infty} N_t(N_\infty - N_t) - \alpha N_t - \beta N_t. \tag{3.3}$$

Rearranging this expression, the dynamical System (3.2) becomes

$$N_{t+1} = (R_0 - \alpha - \beta)N_t - \frac{R_0}{N_\infty}N_t^2, \tag{3.4}$$

defined in the domain $D = [0, N_\infty(R_0 - \alpha - \beta)/R_0]$, with maximal number of infected individuals $N_{\max} = N_\infty (R_0 - \alpha - \beta)^2 / (4 R_0)$.

We have one well defined application $f : D \to D$ if and only if $N_{\max} = N_\infty (R_0 - \alpha - \beta)^2 / (4 R_0) \leq N_\infty(R_0 - \alpha - \beta)/R_0$, which follows, if and only if

$$\alpha + \beta \leq R_0 \leq 4 + \alpha + \beta. \tag{3.5}$$

A straightforward computation shows that the fixed points for (3.2) are given by

$$N_t = 0, \quad N_{R_0} = \frac{N_\infty(R_0 - 1 - \alpha - \beta)}{R_0} \tag{3.6}$$

However, if $\alpha + \beta \leq R_0 \leq 1 + \alpha + \beta$, then there only is one isolated fixed point $N_{R_0} = 0$ in the domain $D$.

The fixed point $N_{R_0}$ (or $N_t = 0$) of the map (3.3) is called *hyperbolic* if the absolute value $|f'(N_{R_0})| \neq 1$ (or $|f'(N_0)| \neq 1$, respectively).

For any initial condition $N_0 \in D$ of the System (3.4), the sequence of points

$$\mathcal{O}_f(N_0) = \{f(N_0), f^2(N_0), f^3(N_0), f^4(N_0), \cdots\} = \{f^k(N_0)\}_{k=1}^{\infty}$$

is called the *orbit of $N_0$ under the the iteration map $f$*. Here, $f^k$ indicates the composition of $f$ with itself $k$ times: $f^k = f \circ f \circ f \cdots \circ f$.

We establish the following result on the stabilization of System (3.4).

**Theorem 1.** *Let $0 < N_0 < \dfrac{N_\infty(R_0 - \alpha - \beta)}{R_0}$ be an initial condition of infected individuals for System (3.2) at time $t = 0 \in \mathbb{N}$. Then,*

*(a) If $\alpha + \beta \leq R_0 \leq 1 + \alpha + \beta$, then orbit $\mathcal{O}_f(N_0)$ is a monotonically decreasing sequence that converges to the disease-free hyperbolic fixed point $N_{R_0} = 0$, i.e., $f^n \to 0$, as $n \to \infty$.*

*(b) If $1 + \alpha + \beta < R_0 \leq 2 + \alpha + \beta$, then orbit $\mathcal{O}_f(N_0)$ is a monotonically sequence that converges to the endemic hyperbolic fixed point $N_{R_0}$, i.e., $f^n(N_0) \to N_{R_0}$, as $n \to \infty$.*

*(c) If $2 + \alpha + \beta < R_0 < 3 + \alpha + \beta$, then orbit $\mathcal{O}_f(N_0)$ is an oscillating (alternately increasing and decreasing) sequence that converges to the endemic hyperbolic fixed point $N_{R_0}$, i.e., $f^n(N_0) \to N_{R_0}$, as $n \to \infty$.*

*Proof.* If we compute the derivative of the generating function (3.3), we obtain

$$f'(N_t) = (R_0 - \alpha - \beta) - \frac{2R_0}{N_\infty}N_t. \tag{3.7}$$

(a) We evaluate the derivative in the unique fixed point $N_{R_0} = 0$, and we obtain

$$f'(0) = R_0 - \alpha - \beta, \tag{3.8}$$

and it follows that $|f'(0)| < 1$, if and only if, $\alpha + \beta \leq R_0 \leq 1 + \alpha + \beta$. This makes that $N_{R_0} = 0$ be an attractor for the system.

By one graphical analysis we obtain that the subset

$$f\left(\left[\frac{N_\infty(R_0 - \alpha - \beta)}{2R_0}, \frac{N_\infty(R_0 - \alpha - \beta)}{R_0}\right]\right) \subset \left[0, \frac{N_\infty(R_0 - \alpha - \beta)^2}{4R_0}\right] \tag{3.9}$$

as we can see in the figure.

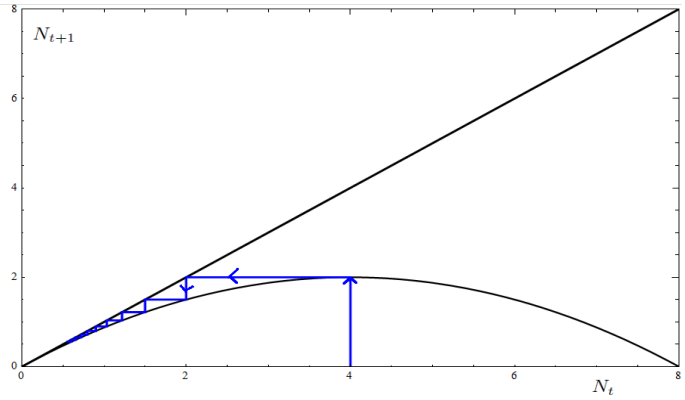


**Figure 1.** Eradication with low capacity of contagion.

Moreover, using the same graphical analysis and condition (3.5), we have that for any initial condition

$$N_0 \in \left[0, \frac{N_\infty(R_0 - \alpha - \beta)^2}{4R_0}\right],$$

its orbit $\{f^n(N_0)\}$ is decreasing and bounded. Therefore, it converges to some point, say $M \in D$. This is,

$$\lim_{n\to\infty} f^n(N_0) = M.$$

Applying again $f$ and using the continuity, we have

$$f(M) = f(\lim_{n\to\infty} f^n(N_0)) = \lim_{n\to\infty} f(f^n(N_0)) = \lim_{n\to\infty} f^{n+1}(N_0)) = M,$$

which implies that $M$ is a fixed point of the system.

Therefore, $M = 0$, since it is the unique fixed point inside the domain $D$, which proves the first item.

(b) If $1 + \alpha + \beta < R_0$, it is easy to see that there are the two aforementioned fixed points (3.6), and evaluating them in the derivative of $f$, we obtain

$$\begin{aligned} f'(0) &= R_0 - \alpha - \beta, \\ f'(N_{R_0}) &= -R_0 + \alpha + \beta + 2. \end{aligned} \tag{3.10}$$

In this way, we have that

$$f'(0) > 1 \quad \Leftrightarrow \quad 1 + \alpha + \beta < R_0,$$

$$|f'(N_{R_0})| \leq 1 \quad \Leftrightarrow \quad 1+\alpha+\beta < R_0 \leq 3+\alpha+\beta. \tag{3.11}$$

In other words, the fixed point $N_0 = 0$ is a repulsive point if $1+\alpha+\beta < R_0$, and the fixed point $N_{R_0}$ is an attractor if $1+\alpha+\beta < R_0 \leq 3+\alpha+\beta$.
For the case $1+\alpha+\beta < R_0 \leq 2+\alpha+\beta$, we have, doing a graphical analysis that once again holds the contention of subsets (3.9).
In this way, from the concavity of the generating function $f$ in the interval $\Omega = \left(0, \frac{N_\infty(R_0-\alpha-\beta)^2}{4R_0}\right)$ (see Figure 2), for any initial condition $N_0 \in \Omega$, there exists one number $0 < \lambda < 1$ such that

$$|f(N_0) - N_{R_0}| = |f(N_0) - f(N_{R_0})| < \lambda |N_0 - N_{R_0}|. \tag{3.12}$$

Applying again $f$, we have

$$|f^2(N_0) - N_{R_0}| = |f(f(N_0)) - N_{R_0}| < \lambda |f(N_0) - N_{R_0}| < \lambda^2 |N_0 - N_{R_0}|, \tag{3.13}$$

and inductively we obtain

$$|f^n(N_0) - N_{R_0}| < \lambda^n |N_0 - N_{R_0}|, \tag{3.14}$$

which implies that orbit $\mathcal{O}_f(N_0)$ converges to the endemic fixed point $N_{R_0}$, i.e., $f^n(N_0) \to N_{R_0}$, as $n \to \infty$. This proves the second item, and it can be seen in Figure 2.

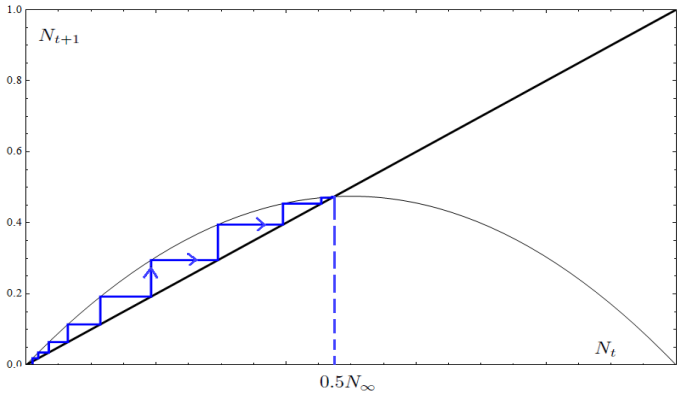


**Figure 2.** Stabilization with suitable capacity of contagion.

(c) For the case $2+\alpha+\beta < R_0 < 3+\alpha+\beta$, let $M_{R_0}$ be the unique point in the interval $\left(0, \dfrac{N_\infty(R_0-\alpha-\beta)}{2R_0}\right)$, such that $f(M_{R_0}) = N_{R_0}$.
We divide the interval

$$\left(0, \frac{N_\infty(R_0-\alpha-\beta)}{R_0}\right) = (0, M_{R_0}) \cup [M_{R_0}, N_{R_0}] \cup \left[N_{R_0}, \frac{N_\infty(R_0-\alpha-\beta)}{R_0}\right).$$

Then, a simple graphical analysis shows that the image $f([M_{R_0}, N_{R_0}])$ is contained in the compact subset $[M_{R_0}, f_{\max}]$.

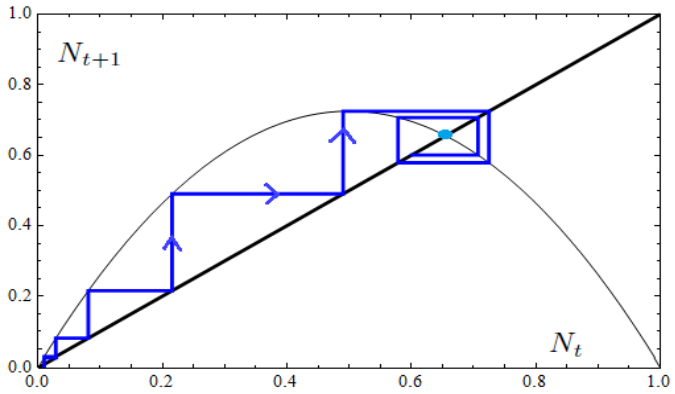


**Figure 3.** Stabilization with small outbreaks and with suitable capacity of contagion.

In a similar way, another graphical analysis shows that

$$f^2\left([M_{R_0}, N_{R_0}]\right) \subset \left[\frac{N_\infty(R_0-\alpha-\beta)}{2R_0}, N_{R_0}\right]$$

as can be seen in the Figure 3.
Therefore, for any initial condition $N_0 \in (M_{R_0}, N_{R_0})$, it follows that $f^2(N_0) \in \left[\frac{N_\infty(R_0-\alpha-\beta)}{2R_0}, N_{R_0}\right]$, and from this point on, the orbit $O_f(N_0)$ is contained in that compact subset. This sequence is oscillating, which converges to the endemic hyperbolic fixed point $N_{R_0}$, as $n \to \infty$.
On the other hand, for any initial condition $N_0 \in (0, M_{R_0})$ there exists one positive integer $k$ such that $f^k(N_0)$ is contained in the subset $[M_{R_0}, N_{R_0}]$, and therefore

$$\lim_{n\to\infty} f^{n+k}(N_0) = N_{R_0}.$$

Since

$$f\left(\left[N_{R_0}, \frac{N_\infty(R_0-\alpha-\beta)}{R_0}\right]\right) \subset (0, N_{R_0}),$$

for any initial condition $N_0 \in \left[N_{R_0}, \frac{N_\infty(R_0-\alpha-\beta)}{R_0}\right]$, its orbit $O_f(N_0)$ converges to the endemic hyperbolic fixed point $N_{R_0}$, as shown in Figure 3.

This ends the proof. □

## 4. Proof of Result 1

In this subsection we will carry out an initial study of prevention for the pandemic in the state of Mexico, since its beginning in April of 2020, assuming that there was no mitigation action since then until now and that the parameters remain constant in all this period. We will continue considering the number of inhabitants of the state of Mexico as constant and equal to $N_\infty$, conforming to a closed population.

In order to understand the pandemic in the state of Mexico, we have obtained data from June of 2020 until September of 2021 from [24] and we have provided tables of contagion, mortality and rates of mortality, as shown in Appendix A.

We have obtained, by computing the mean from the early data, the following initial constant values for the parameters at the beginning of the pandemic in the state of Mexico, in the period of 2020–2021.

$$R_0 = 2, \quad \alpha = 0.20, \quad \beta = 0.19,$$

and therefore, the generating function for dynamics becomes

$$f(N_t) = 1.61N_t - \frac{2}{N_\infty}N_t^2$$

where the domain for the pandemic is

$$D = \left[0, \frac{N_\infty (2 - 0.2 - 0.19)}{2}\right] = [0, 0.80N_\infty],$$

which indicates that, with this model, only 80 percent of the population $N_\infty$ of the state of Mexico faced the epidemic.

The maximum number of infected individuals should be

$$N_{max} = \frac{N_\infty (2 - 0.2 - 0.19)^2}{4\,(2)} = 0.324N_\infty,$$

that is, the maximum number of infected individuals should be 32.4 percent of the population $N_\infty$ of the state of Mexico.

The fixed points for the system obtained are

$$N_t = 0 \quad \text{(disease-free hyperbolic fixed point).}$$

and

$$N_{R_0} = \frac{N_\infty (2 - 1 - 0.2 - 0.19)}{2} = 0.30N_\infty \quad \text{(endemic hyperbolic fixed point)}$$

From Theorem 1, with $R_0 = 2$, we are in the case

$$1 + \alpha + \beta < R_0 \leq 2 + \alpha + \beta,$$

$$1.39 < 2 \leq 2.39,$$

and therefore, for any initial condition $N_0 \in D$, its orbit $O_f(N_0)$ converges to the endemic fixed point $N_{R_0}$, i.e., $f^n(N_0) \to 0.30N_\infty$ as $n \to \infty$, which is shown in Figure 4.

This indicates that the epidemic stabilizes at a fixed point associated with the number of infected being 30 percent of the total population $N_\infty$ of the state of Mexico.

In other words, the epidemic would have been stabilized (called "flattening the contagion curve") in a natural way with these conditions if they did not change, both the basic contagion number and the recovery and mortality parameters. This ends the proof of Theorem 1.

However, this was not the case, and although the statistical data have shown for fortnightly periods that the basic reproductive number $R_0 < 1$, the pandemic continues. We will discuss this in a later section.

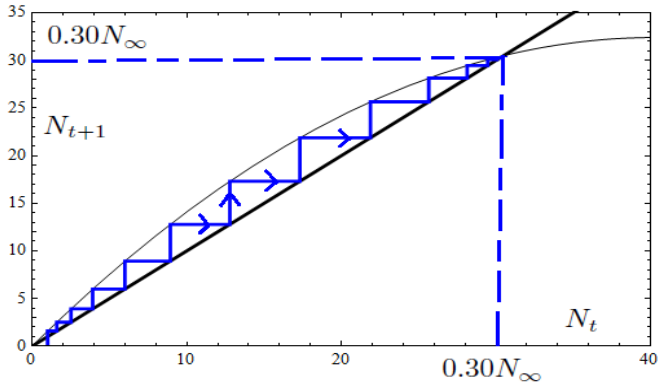


**Figure 4.** Stabilization in state of Mexico with suitable capacity of contagion.

## 5. Chaotic dynamical systems

To the aim of taking into account more values of $R_0$, we note that System (3.2) makes sense for the problem in the case of a domain $D$ when $\alpha + \beta \leq R_0 \leq 4 + \alpha + \beta$.

Another direct calculation shows us that if

$$3 + \alpha + \beta < R_0 \leq 4 + \alpha + \beta, \tag{5.1}$$

then $f'(N_{R_0}) < -1$, which yields the fixed point $N_{R_0}$ being repulsive for System (3.2), as well as $N_t = 0$.

In this case, we have a possibly chaotic dynamics, which is due to compactness of the domain $D$ and also to the fact that the orbit of any initial condition is repelled by both fixed points.

Let us introduce the following definitions [25].

**Definition 1.** *A point $N_{R_0} \in D$ is said to be periodic of (prime) period $k \geq 1$ for the System (3.3) if its orbit is finite of k-elements. That is, $f^k(N_{R_0}) = N_{R_0}$ and $f^i(N_{R_0}) \neq N_{R_0}$ for $i \leq k - 1$ (i.e, the least positive is k).*

In other words, a $k$-periodic point of System (3.3) is a fixed point of the iterate $f^k$. In particular, a fixed point is 1-periodic, and so it is periodic of all the orders.

**Definition 2.** *Let $N_{R_0} \in D$ be a periodic point of prime period k. The point $N_{R_0}$ is called hyperbolic if $|(f^k)'(N_{R_0})| \neq 1$. The number $(f^k)'(N_{R_0})$ is called the multiplier of the periodic point.*

An important result toward finding simple conditions to characterize a chaotic system is given next [25].

**Theorem 2.** *(Sarkovskii) Let $f : D \subset \mathbb{R} \to D \subset \mathbb{R}$ be a continuous function defined in a compact interval D, such that it has a periodic point of period three. Then, $f$ has periodic points of all periods.*

Let us introduce our last definition [25].

**Definition 3.** *Let $f : D \to D$ be a continuous function associated with a discrete dynamical system*

$$N_{t+i} = f(N_t). \tag{5.2}$$

*We say the following.*

1. *$f$ is topologically transitive if for any open interval $U \subset D$ its orbit $\{f^n(U)\}$ intersects any other open interval $V \subset D$.*
2. *$f$ is sensibly dependent to initial conditions if for any pair of points closed to the same open set $N_t, N_s \in U \subset D$, the corresponding orbits $\{f^n(N_t)\}, \{f^n(N_s)\}$ depart from each other after some value $n \geq 1$.*

**Definition 4.** *Let $f : D \subset \mathbb{R} \to D \subset \mathbb{R}$ be a continuous function defined in a compact interval $D$. We say that the one-dimensional dynamical System (5.2) is chaotic if it satisfies the conditions from Definition 3, and the periodic points of $f$ are dense in $D$.*

The fundamental result which we will use in this work is due to Li and Yorke [26], and we state it as follows.

**Theorem 3.** *(Li-Yorke) Let $f : D \subset \mathbb{R} \to D \subset \mathbb{R}$ be a continuous function defined in a compact interval $D$, such that it has a periodic point of period three. Then, the one-dimensional dynamical System (5.2) defined by $f$ is chaotic.*

In this way, showing that the Covid-19 pandemic might have chaotic behaviors, for certain values of the involved parameters, reduces to finding a periodic point of period three. This is shown in the next section.

## 6. Weak chaotic mitigation of the Covid-19 pandemic via data in the state of Mexico

In the time period studied, before vaccines and/or effective treatments were created to fight this disease, the only available control measures were lockdown, quarantine, etc. Indeed, in [22] it is said that applying mitigation strategies seems to decrease an initial $R_0$ (at time $t = 0$). Then, $R$ (as a parameter) acts as one of the few available observable control measures in the curtailing of this disease.

Let us represent System (3.2) as the following affine control system:

$$N_{t+1} = f_1(N_t) + f_2(N_t)\, R = -(\alpha N_t + \beta N_t) + N_t \left(1 - \frac{N_t}{N_\infty}\right) R, \tag{6.1}$$

where the parameter $R$ is taken as one control input. Hereafter, we propose $R = R(t) = R_t$ as a time-dependent control, the values of which are the estimated values of $R$, according to the adopted mitigation measures.

The aim of this section is to address how to eradicate the Covid-19 epidemic by regulating the contagion capacity, which will depend on discrete time units. In specific, we will provide conditions for the contagion capacity to decrease through a difference equation $R_{t+1} = g(R_t)$, with $g(R_t)$ a smooth enough map, defined in the interval $[0, 4 + \alpha + \beta]$, so that its solution decreases per unit of time and in turn leads to eventually eradicating the disease.

We shall call from now on the smooth function $g : [0, 4 + \alpha + \beta] \to [0, 4 + \alpha + \beta]$ *the mitigation map*.

Let us take the one dimensional discrete dynamical System (6.1) together with the difference equation $R_{t+1} = g(R_t)$ as the following two-dimensional *non-linear discrete dynamical system*:

$$\begin{cases} N_{t+1} &= (R_t - \alpha - \beta)N_t - \frac{R_t}{N_\infty} N_t^2, \\ R_{t+1} &= g(R_t), \end{cases} \tag{6.2}$$

defined in the rectangular set $\hat{D} = [0, N_\infty(R_0 - \alpha - \beta)/R_0] \times [0, 4 + \alpha + \beta]$.

Let $R_t = R(t)$ be a smooth function, obtained by integrating the discrete equation, $R_{t+1} = g(R_t)$, for $g$ a smooth mitigation map defined in the interval $[0, 4 + \alpha + \beta]$.

With data for the basic number of contagion $R_t$ in the state of Mexico obtained from the AMMA model of CONACYT, Mexico [27], in the months of April, May, June, August, September and October of 2020, which are shown in Appendix B, we have in fortnights the quartic polynomial function

$$g(R_t) = 1.8607R_t^5 - 17.355R_t^4 + 47.874R_t^3 - 51.806R_t^2 + 20.026R_t$$

in the variable $R_t$ by interpolating the points in the plane $(R_t, R_{t+1})$

$$(1.7, 1),\ (1.4, 1.2),\ (0.7, 1.2),\ (1.2, 0.8),\ (1.0, 0.6),\ (0, 0).$$

This polynomial fits (with a very good approximation) this process in the well observed interval of data for the capacity of contagion $[0.6, 1.6]$, which is a suitable interval for mitigation contained in the total interval of mitigation $[0, 4.39]$, as can be seen in Figure 5.

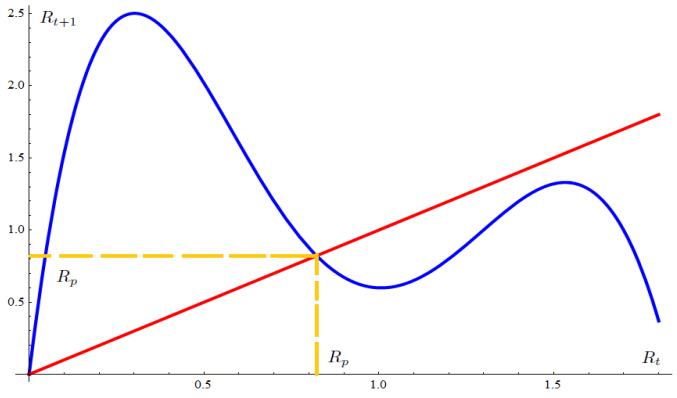


**Figure 5.** Function of mitigation $g$ in Months of April, May, June, August, September and October of 2020.

The fixed point in that interval is $R_p = 0.822$, and since

$$g'(R_t) = 9.3035R_t^4 - 69.42R_t^3 + 143.322R_t^2 - 103.612R_t + 20.026,$$

$|g'(R_p)| = |g'(0.822)| = |-2.4| = 2.4$.

Therefore, in the global interval $[0, 4.39]$ there are two repulsive fixed points, at $R_t = 0$ and $R_p = 0.822$. Further, the derivative satisfies $|g'(R_p)| \geq 1$.

The dynamics of the system

$$R_{t+1} = 1.8607R_t^5 - 17.355R_t^4 + 47.874R_t^3 - 51.806R_t^2 + 20.026R_t \tag{6.3}$$

in the aforementioned interval $[0.6, 1.6]$ for the initial condition $R_0 = 0.7$ can be seen in Figure 6.

On the other hand, a long but straight forward computation shows us the existence of the eight points of period three of $g$ which we list above,

$$0.0,\quad 0.6601,\quad 0.6871,\quad 0.8242,\quad 0.8942,\quad 1.109,\quad 1.246,\quad 1.348.$$

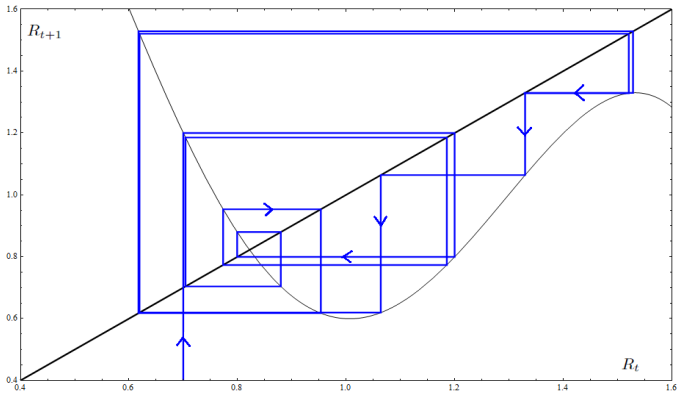


**Figure 6.** Dynamics for the initial condition $R_0 = 0.7$.

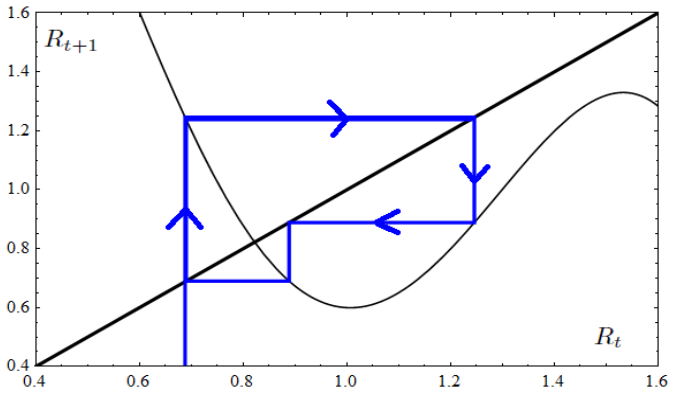


**Figure 7.** The point $R_t = 0.6878$ is a 3-periodic point for $g$.

In fact, the point $R_t = 0.6871$ is a periodic point of period 3 for the map $g$, as it can be obtained by the aforementioned computation, and its orbit is shown in the Figure 7.

By the Sarkovskii's Theorem [25], there is a dense set of periodic points of all periods for this mitigation function. Consequently, by the Yorke and Li Theorem [25], the map $g$ is chaotic, as shown in Figure 6.

## 7. Proof of Result 2

The System (6.2), with this mitigation function, becomes

$$\begin{cases} N_{t+1} &= f(N_t, R_t) = (R_t - 0.39)N_t - \frac{R_t}{N_\infty}N_t^2, \\ R_{t+1} &= g(R_t) = 1.8607R_t^5 - 17.355R_t^4 + 47.874R_t^3 - 51.806R_t^2 + 20.026R_t, \end{cases} \tag{7.1}$$

and it will be analyzed in the observable domain $\Omega = [0, 0.8N_\infty] \times [0.6, 1.6]$.

The obtained dynamical relation is very difficult to integrate to obtain a time-dependent mitigation relationship $R = R(t)$, and it will be qualitatively used to display results on the first coordinate of System (7.1).

As before, we assume still a closed population with a total number of individuals $N_\infty$.

In order to study the dynamics of (7.1), first, we obtain the fixed points of System (7.1) by solving the algebraic system of equations

$$\begin{cases} N_t &= (R_t - \alpha - \beta)N_t - \frac{R_t}{N_\infty}N_t^2, \\ R_t &= 1.8607R_t^5 - 17.355R_t^4 + 47.874R_t^3 - 51.806R_t^2 + 20.026R_t, \end{cases} \tag{7.2}$$

which gives us the points $p_1 = (0, 0)$ and $p_2 = (0, R_p) = (0, 0.822)$ in the whole set $\Lambda = [0, 0.8N_\infty] \times [0, 4.39]$.

We begin by defining the 2-real valued map

$$F(N_t, R_t) = \Big((R_t - \alpha - \beta)N_t - R_t\, N_t^2/N_\infty,\ g\,(R_t)\Big) \tag{7.3}$$

in $\Lambda$, whose iterates determine the orbits of the System (7.1) as $(N_{t+1}, R_{t+1}) = F(N_t, R_t)$.

In this case, the Jacobian of (7.3) is

$$DF_{(N_t,R_t)} = \begin{pmatrix} R_t - 0.39 - \frac{2R_tN_t}{N_\infty} & N_t - \frac{N_t^2}{N_\infty} \\ 0 & g'(R_t) \end{pmatrix}, \tag{7.4}$$

and here $(')$ denotes the ordinary derivative with respect to $R_t$.

**a.** Therefore, the Jacobian matrix at the point $p_1 = (0, 0)$ is

$$DF_{(0,0)} = \begin{pmatrix} -0.39 & 0 \\ 0 & g'(0) \end{pmatrix}. \tag{7.5}$$

A straightforward computation gives us the eigenvalues, $\mu_1 = -0.39$, which in absolute value is less than 1, and $\mu_2 = 20.02$, which is great than 1.

It is easy to see that the coordinate axis $R_t$ is an invariant under the System (7.1), which follows from the equality

$$F(0, R_t) = (0, g\,(R_t)), \tag{7.6}$$

That invariance of the axis $R_t$, implies that in this direction $p_1$ is a repulsive point for all the orbits close to this fixed point with initial conditions $(0, R_0)$. A similar analysis shows that the axis $N_t$ (where $R_t = 0$) is also invariant under System (6.2), which follows from the equality

$$F(N_t, 0) = (-0.39N_t, 0). \tag{7.7}$$

Therefore, any orbit with initial conditions $(N_0, 0)$ converges to the point $p_1 = (0, 0)$, along this axis.

We conclude that the fixed point $p_1 = (0, 0)$ is a *saddle fixed point for the system*.

**b.** For the fixed point $p_2 = (0, R_p) = (0, 0.822)$, we have the Jacobian matrix

$$DF_{(0,R_p)} = \begin{pmatrix} 0.432 & 0 \\ 0 & -2.4 \end{pmatrix}, \tag{7.8}$$

whose eigenvalues are $\mu_1 = 0.432$, which in absolute value is less that 1, and $\mu_2 = -2.4$, which in absolute value is great that 1. This implies that such point is also a *saddle fixed point* for the system.

We remark that the straight line $R_t = R_p = 0.822$, (where $g(R_p) = R_p$) is also an invariant set under System (6.2), which follows from the equality

$$F(N_t, 0.822) = \left(0.432N_t - N_t^2/N_\infty, 0.822\right) \tag{7.9}$$

which implies that any orbit with initial conditions $(N_0, 0.822)$ in such line converges to the fixed point $p_2 = (0, 0.822)$.
It follows that the stable manifold for $p_2 = (0, R_p)$ is the set $W^s(R_p) = \Lambda \setminus \{R_t = 0\}$ [25,28].

On the other hand, from the invariance of the axis $R_t$, any orbit with initial conditions $(0, N_0)$ remains in such axis, preserving the dynamics of System (6.3).
We observe that the aforementioned mitigation map turns the System (7.1) for this case into a *weak chaotic* one. That is, the whole system is not chaotic in the sense of Li and Yorke [25], but, as we have mentioned before, it is chaotic in the sense of Li and Yorke only in the vertical coordinate $R_t$, and this makes unpredictable the convergence of the system's orbits for any initial condition $(N_0, R_0)$ which is not contained on the invariant coordinate axes or on the also invariant line $R_t = R_p$. We shall consider this type of system to be *weak chaotic* [16].

It is well known that, in general, a manifold, whether stable or unstable, is not a differentiable manifold in the sense of differential topology, but sometimes they are unions of pieces of differentiable manifolds. For the case of planar maps, sometimes one dimensional manifolds are unions of piecewise smooths curves [29].

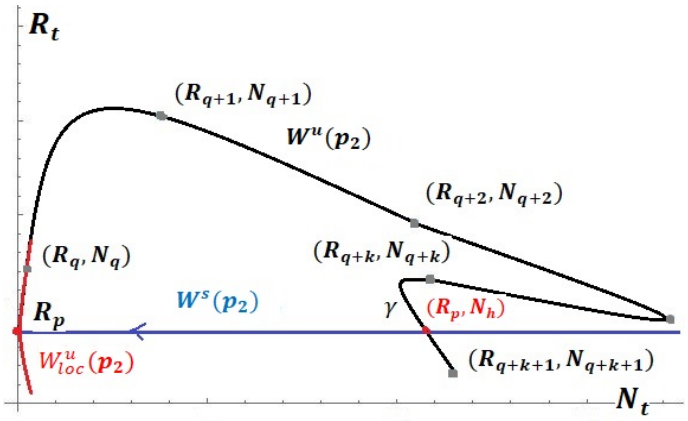


**Figure 8.** Intersection of the invariant manifolds $W^u(p_2)$ and $W^s(p_2)$ in the homoclinic point $(R_p, N_h)$.

The one dimensional unstable manifold $W^u(p_2)$ of System (7.1) at the point $p_2$ is not the $R_t$-axis because by Sarkovskii's Theorem and in any neighborhood of $p_2$ the subset of periodic point is dense and all those orbits returns to that neighbourhood. We note that the local stable manifold $W^u_{\text{loc}}(p_2)$ is also not contained in the $R_t$-axis for the same reason. The one dimensional (curve) unstable manifold $\gamma = W^u(p_2)$ is found by iterating the local unstable manifold $W^u_{\text{loc}}(p_2)$ using the technique of Yorke *et al.* in [30] (Figure 8).
Following the proof of Theorem 3 in [16], we can show that the one dimensional unstable and the stable global invariant manifolds $W^u(p_2)$ and $W^s(p_2)$ intersect transversally. Therefore, System

(7.1) has transverse homoclinic points. Moreover, we can obtain a vertical "homoclinic tangle", and a high enough forward iterate of $F$ in the obtained vertical "homoclinic tangle" will give us a vertical Smale horseshoe map [25, 28, 31] (Figure 8).

However, since the set intersection between the stable $W^s(p_2)$ and unstable $W^u(p_2)$ manifolds at point $p_2$ has zero dimension and therefore zero Lebesgue measure, in topological and measurable terms, we can, summarizing the previous discussion, establish the following main result.

**Theorem 4.** *The mitigation System (7.1) is vertically chaotic near the eradication point* $p_2 = (0, R_p) = (0, 0.822)$. *Therefore, although it is globally weak chaotic, the system eradicates slowly the pandemic for almost all (in the topological and measurable senses) initial conditions.*

In fact, the generic behavior of the dynamical system is shown discretely in Figure 9.

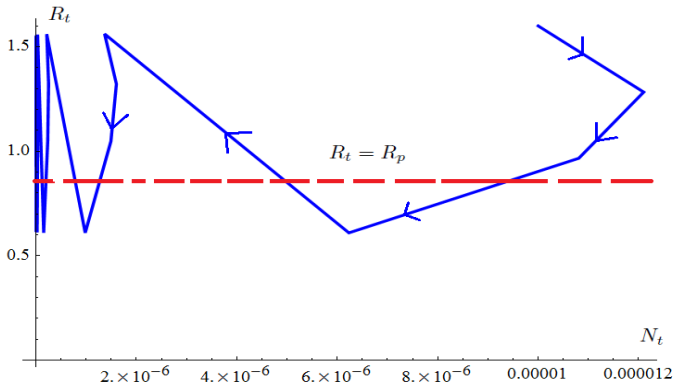


**Figure 9.** Chaotic eradication beginning with initial suitable capacity of contagion.

The expected behavior of the actual infected function $N(t) = N_t$ as a function of the time $t$ measured in fortnights for the first 13 units since April 2020 is shown in Figure 10, and the eradication of the pandemic would have been expected during that period of time, according to the data obtained and mentioned above.

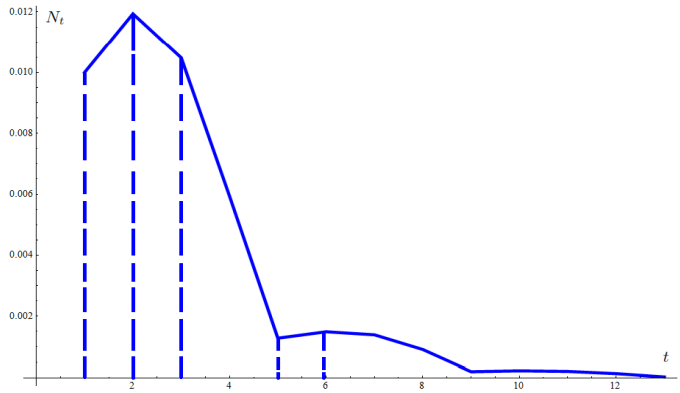


**Figure 10.** Behaviour of the function $N_t$ in the first 13 fortnights since April 2020.

On the other hand, the expected actual capacity of the contagion function $R(t) = R_t =$, also as a

function of the time $t$ measured in fortnights for the first 15 fortnights since April 2020, is shown in Figure 11. This function has a chaotic behavior throughout the period, which causes the $N(t)$ function to show a slow eradication trend. This ends the proof of Theorem 2.

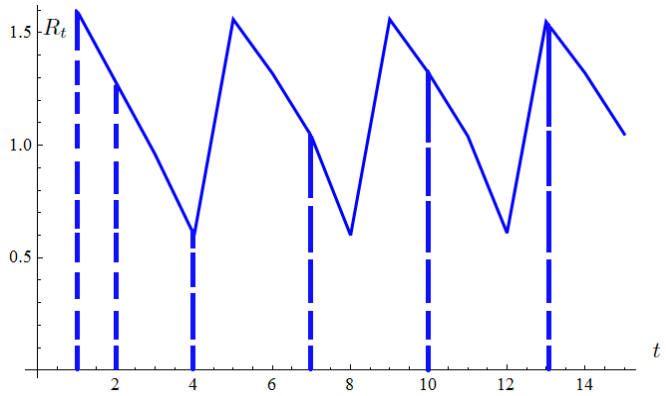


**Figure 11.** Behavior of the function $R_t$ in the first 15 fortnights since April 2020.

## 8. Conclusions

The two-dimensional model defined by a discrete dynamic system and built with the statistical data obtained from the mentioned sources shows us that, for almost all initial conditions in the number of infected and in the basic number of infection, the eradication of the pandemic would have been possible, if we had been conserved, the conditions of contagion (variable), recovery and mortality (constant) even when the mitigation had a chaotic behavior by fortnightly units. However, the behavior of the epidemic for the following variants in 2021 and 2022 followed a similar way, but they are still having repercussions on the economy and social, health and political aspects. In a particular conclusion, the mitigation and prevention strategy in the State of Mexico followed only economic and health objectives, neglecting social aspects (mental health, divorces, femicides, etc.) and influencing political problems (through political parties, opposition to the current Mexican government, as well as the problem of sale and distribution of vaccines, social movements, etc.).

## Acknowledgments

The authors would like to thank the Tecnologico de Estudios Superiores de Huixquilucan (TESH) and the Consejo Mexiquense de Ciencia y Tecnología (COMECYT) for the financial support to carry out this research. Also, the authors thank to mathematician Hiram Velásquez Alamilla from UAM-I, for his support in giving this paper its final Tex format.

## Conflict of interest

The authors declare there is no conflict of interest.

## References


1. M. Coccia, Pandemic prevention: Lessons from COVID-19 pandemic, *Encyclopaedia*, **1** (2021), 433–444. https://doi.org/103390/Encyclopaedia1020036
2. M. Coccia, High health expenditures and low exposure of population to air pollution as critical factors that can reduce fatality rate in COVID-19 pandemic crisis: A global analysis, *Environ. Res.*, **199** (2021), 111339. https://doi.org/10.1016/j.envrers.2021.111339
3. M. Coccia, Preparedness of countries to face COVID-19 pandemic crisis: Strategic position and underlying structural factors to support strategies of prevention of pandemic threats, *Environ. Res.*, **203** (2022), 111678. https://doi.org/10.1016/j.envrers.2021.111678
4. M. Coccia, COVID-19 pandemic crisis over 2020 (with lock downs) and 2021 (with vaccinations): Similar effects for seasonality and environmental factors, *Environ. Res.*, **208** (2022), 112711. https://doi.org/10.1016/j.envrers.2022.112711
5. X. Chen, B. Yu, First two months of the 2019 Corona virus Disease (COVID-19) epidemic in China: Realtime surveillance and evaluation with a second derivative model, *Global Health Res. Policy*, **5** (2020). https://doi.org/10.1186/s41256-020-00137-4
6. F. Louchet, A brief theory of epidemic kinetics, *Biology*, **9** (2020), 134. https://doi.org/10.3390/biology9060134
7. A. Nunez-Delgado, E. Bontemoi, M. Coccia, M. Kumar, K. Farkas, J. L. Domingo, SARS-COV-2 and other pathogenic micro-organisms in the environment, *Environ. Res.*, **201** (2021), 111606. https://doi.org/10.1016/j.envrers.2021.111606
8. S. Sanche, Y. T. Lin, C. Xu, E. Romero-Severson, N. Hengartner, R. Ke, High contagiousness and rapid spread of severe acute respiratory syndrome coronavirus 2, *Emerg. Infect. Dis.*, **26** (2020), https://doi.org/10.3201/eid2607.200282
9. W. Kermack, A. McKendrick, A contribution to the mathematical theory of epidemics, *Proc. Royal Soc. A.*, **115** (1927), 700–721. https://doi.org/10.3201/eid2607.200282
10. M. Canals, C. Cuadrado, A. Canals, COVID-19 in Chile: The usefulness of simple epidemic models in practice, *Medwave*, **8119** (2021). https://doi.org/10.5867/medwave.2021.01.8119
11. T. S. Fernandes, Chaotic model for COVID-19 grow factor, *Res. Biomed. Eng.*, **38** (2022), 299–303. https://doi.org/10.1007/s42600-020-00077-5
12. J. Guo, A. Wang, W. Zhou, Y. Gong, S. R. Smith, Discrete epidemic modelling of COVID-19 transmission in Shaanxi Providence with media reporting and imported caes, *Math. Biosci. Eng.*, **19** (2022), 1388–1410. https://doi.org/10.3934/mbe.2022064
13. M. T. Li, G. Q. Sun, J. Zhang, Y. Zhao, X. Pei, L. Li, et al., Analysis of COVID-19 transmission in Shanxi Province with discrete time imported cases, *Math. Biosci. Eng.*, **17** (2020), 3710. https://doi.org/10.3934/mbe.2020208
14. A. Mourad, F. Mroue, Z. Taha, Stochastic mathematical models for the spread of COVID-19: A model epidemiological approach, *Math. Med. Biol.*, **39** (2022), 49–76. https://doi.org/10.1093/imammb/dqab019

15. T. Sitthiwirattham, A. Zeb, S. Chasreechai, M. Tilioua, S. Djilail, Analysis of a discrete mathematical COVID-19 model, *Results Physicsy*, **28**, (2021), 104668. https://doi.org/10.1016/j.rinp.2021.104668
16. J. G. Reyes-Victoria, J. Solis-Daun, L. Herrera-Zuniga, E. Vázquez-Jiménez, Discrete model for prevention of Covid-19 Pandemic for closed populations: Stabilization, eradication and weak chaos, preprint, 2022.
17. E. Callaway, Fast spreading COVID-19 variant can elude immune responses, *Nature*, **589** (2021), 500–5001. https://doi.org/10.1038/d41586-021-00121-z
18. E. B. Postnikov, Estimation of COVID-19 dynamics "on a back-of-envelop": Does the simplest SIR model provide quantitative parameters and predictions?, *Chaos Solitons Fractals*, **135** (2020), 109841. https://doi.org/10.1016/j.chaos.2020.109841
19. C. Aschwanden, Five reasons why COVID-19 heard immunity is probably impossible, *Nature*, **591** (2021), 520–522. https://doi.org/10.1038/d41586-021-00728-2
20. J. G. Reyes-Victoria, J. Solis-Daun, L. Herrera-Zuniga, Epidemic model as an aid to control decision-making in the Covid-19 Pandemic for closed populations: Qualitative analysis and Chaos, *COVID-19 Res. Commun.*, 2020.
21. Z. Cao, Q. Zhang, X. Lu, D. Pfeiffer, Z. Jia, H. Song, et al., Estimating the effective reproduction number of the 2019-nCoV in China, *Biology*,(2020). https://doi.org/10.1101/2020.01.27.20018952
22. Y. Liu, A. Gayle, A. Wilder-Smith, J. Rocklöv, The reproductive number of COVID-19 is higher compared to SARS coronavirus, *J. Travel Med.*, **27** (2020), 1–4. https://doi.org/10.1093/jtm/taaa021
23. R. May, Simple mathematical models with very complicated dynamics, *Nature*, **261** (1976), 459–467. https://doi.org/10.1038/261459a0
24. *John Hopkins University*, Medicine, 2020. Available from: https://coronavirus.jhu.edu/map.html.
25. R. Devaney, *An Introduction to Chaotic Dynamical Systems*, $2^{nd}$ edition, Addison-Wesley, USA, 1989.
26. T. Y. Li, J. Yorke, Period three implies chaos, *The Amer. Math. Monthly*, **82** (1975), 985–992. https://doi.org/10.1007/978-0-387-21830-4_6
27. A. Christen, M. Capistán, M. Daza-Torres, A. Capella *Instituto de Matemáticas UNAM, U.C. DAVIS, CIMAT-CONACYT, CONACYT, Gobierno de México*, (82:10) , (2020-2021).
28. J. Guckenheimer, P. Holmes, *Nonlinear Oscillations, Dynamical Systems, and Bifurcations of Vector Fields*, $1^{st}$ edition, Springer, New York, 1983.
29. R. McGehee, A stable manifold theorem for degenerate fixed points with applications to celestial mechanics, *J. Differ. Equations*, **14** (1973), 70–88. https://doi.org/10.1016/0022-0396(73)90077-6
30. E. Zhipingyou, E. Kostelich, J. Kostelich, J. Yorke, Calculating stable and unstable manifolds, *Int. J. Bifurcation Chaos*, **1** (2012). https://doi.org/10.1142/S0218127491000440
31. J. Palis, W. De Melo, *Geometric Theory of Dynamical Systems*, $1^{st}$ edition, Springer-Verlag, New York, 1982.

## Appendix A

We show here the obtained data from June of 2020 until September of 2021, from [24], providing the tables of contagion, mortality and the corresponding rates in the state of Mexico.

**Table A1.** Data from June of 2020 to September of 2021 of contagion of COVID-19.

| Fortnight | Mean of Contagious |
|---|---|
| 15-jun | 606.9 |
| 1-jul | 680.9 |
| 15-jul | 663.6 |
| 1-ago | 538.6 |
| 15-ago | 547.2 |
| 1-sep | 439.2 |
| 15-sep | 456.1 |
| 1-oct | 426.5 |
| 15-oct | 639.1 |
| 1-nov | 478.6 |
| 15-nov | 365.5 |
| 1-dic | 528.7 |
| 15-dic | 994.9 |
| 1-ene | 1210.1 |
| 15-ene | 1097.1 |
| 1-feb | 1788.2 |
| 15-feb | 999.6 |
| 1-mar | 782.7 |
| 15-mar | 624.6 |
| 1-abr | 463.4 |
| 15-abr | 413.8 |
| 1-may | 309.6 |
| 15-may | 197 |
| 1-jun | 186.53 |
| 15-jun | 315.57 |
| 1-jul | 291.06 |
| 15-jul | 601.07 |
| 1-ago | 1395.35 |
| 15-ago | 1670.71 |
| 1-sep | 1227.76 |

**Table A2.** Data from June of 2020 to August of 2021 of Mean of Mortality, and the rates in the state of Mexico by COVID-19.

| Fortnight | Mean of Mortality | M. Mortality/M. Contagious |
|---|---|---|
| 21-jun. | 68.1 | 0.11 |
| 07-jul | 140.8 | 0.21 |
| 21-jul | 66.7 | 0.10 |
| 07-ago | 63.5 | 0.12 |
| 21-ago | 54.8 | 0.10 |
| 07-sep | 43.1 | 0.10 |
| 21-sep | 48.8 | 0.11 |
| 07-oct | 60.9 | 0.14 |
| 21-oct | 25.8 | 0.04 |
| 07-nov | 34.5 | 0.07 |
| 21-nov | 297.9 | 0.82 |
| 07-dic | 516.1 | 0.98 |
| 21-dic | 102.2 | 0.10 |
| 07-ene | 126.5 | 0.10 |
| 21-ene | 169.9 | 0.15 |
| 07-feb | 209.2 | 0.12 |
| 21-feb | 155.1 | 0.16 |
| 07-mar | 123.1 | 0.16 |
| 21-mar | 80.9 | 0.13 |
| 07-abr | 75.6 | 0.16 |
| 21-abr | 114.2 | 0.28 |
| 07-may | 40.4 | 0.13 |
| 21-may | 32.2 | 0.16 |
| 07-jun | 144 | 0.77 |
| 21-jun | 13.4 | 0.04 |
| 07-jul | 17.3 | 0.06 |
| 21-jul | 20.4 | 0.03 |
| 07-ago | 54.8 | 0.04 |
| 21-ago | 87.4 | 0.05 |

## Appendix B

The data for the basic numbers of contagion $R_t$ in the state of Mexico obtained from the AMMA model of CONACYT, Mexico [27], in the months of April, May, June, August, September and October of 2020, give the following quantities in fortnights, as can be seen in the figures below.

- From $R_t = 1.7$ on 28th April to $R_{t+1} = 1.0$ on 27th May (see Figure A1).
- From $R_t = 1.4$ on 28th may to $R_{t+1} = 1.2$ on 26th June (see Figure A2).
- From $R_t = 0.7$ on 27th August to $R_{t+1} = 1.2$ on 24th September (see Figure A3 ).

– From $R_t = 1.2$ on 09th September to $R_{t+1} = 0.8$ on 08th October (see Figure A4).
– From $R_t = 1.0$ on 23th September to $R_{t+1} = 0.6$ on 22th October (see Figure A5).

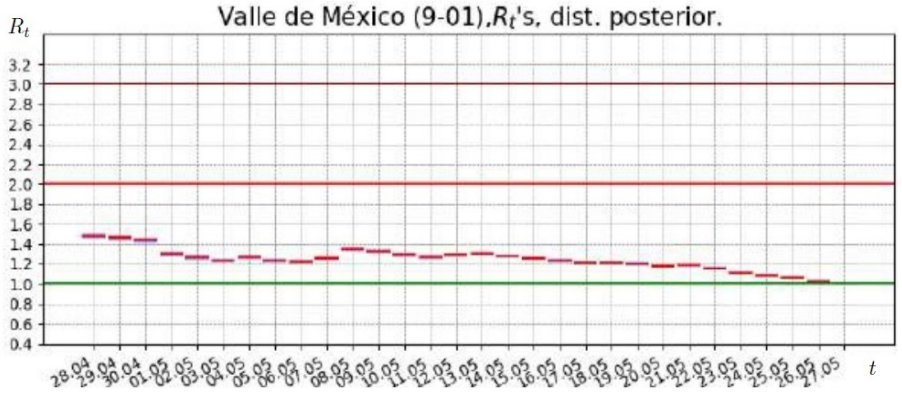


**Figure A1.** Data of mitigation AMMA in Months of April and May of 2020.

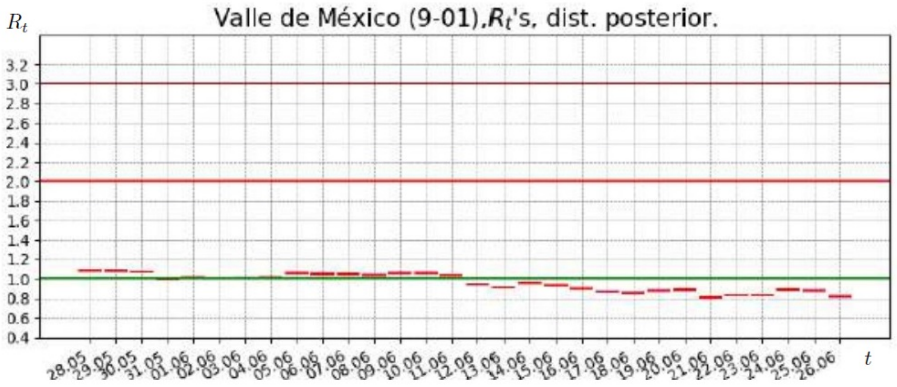


**Figure A2.** Data of mitigation AMMA in Months of May and June of 2020.

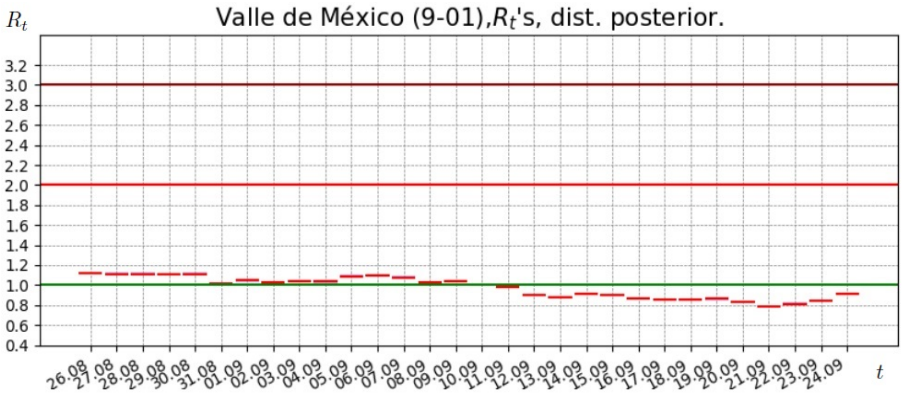


**Figure A3.** Data of mitigation AMMA in Months of August-September of 2020.

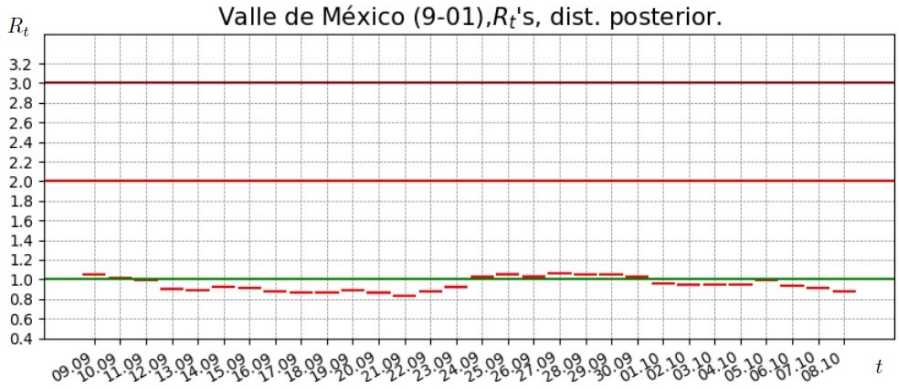


**Figure A4.** Data of mitigation AMMA in Months of September-October of 2020.

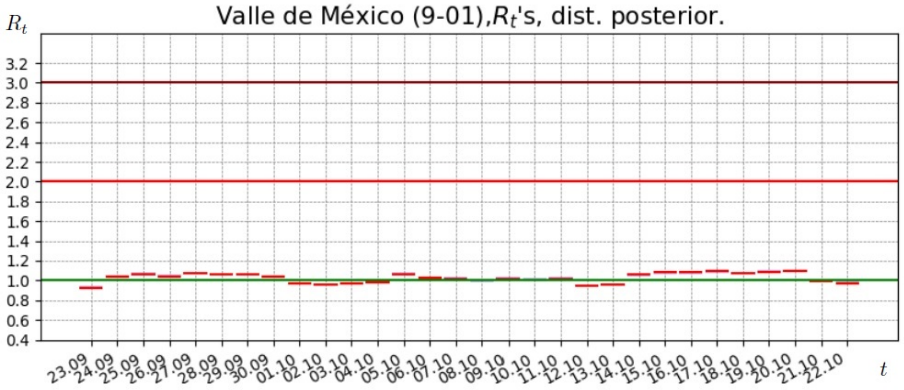


**Figure A5.** Data of mitigation AMMA in Months of September and October of 2020.